

THE “BALDWIN EFFECT” IN WOLF-RAYET STARS

PATRICK MORRIS AND PETER S. CONTI

Joint Institute for Laboratory Astrophysics, Campus Box 440, University of Colorado, Boulder, CO 80309-0440

HENNY J. G. L. M. LAMERS

Astronomical Institute and SRON Laboratory for Space Research, Sorbonnelaan 2, 3584 CA Utrecht, The Netherlands

AND

GLORIA KOENIGSBERGER

Instituto de Astronomia, UNAM, Apdo. Postal 70-264, México, D.F. 04510, México

Received 1993 March 29; accepted 1993 June 14

ABSTRACT

The equivalent widths of a number of emission lines in the spectra of WN-type Wolf-Rayet stars are found to inversely correlate with the luminosity of the underlying continuum. This is the well-known Baldwin Effect that has previously been observed in quasars and some Seyfert I galaxies. The Effect can be inferred from line and continuum predictions in published non-LTE model helium atmospheres and is explainable in terms of differences in wind density among WN stars. Using a simple wind model, we show that the Effect arises from the fact that both the effective radius for the local continuum and the emission measure of the layers above the continuum-forming region depend on the density in the wind. The Effect provides a new method for distance determinations of W-R stars.

Subject headings: galaxies: active — line: formation — quasars: emission lines — stars: atmospheres — stars: Wolf-Rayet

1. INTRODUCTION

Ultraviolet studies of quasar emission-lines have shown that the equivalent width of the C IV $\lambda 1550$ emission feature inversely correlates with the luminosity of the underlying continuum (Baldwin 1977; Baldwin et al. 1978; Wampler et al. 1984, hereafter WGBB; Kinney et al. 1985, 1987; Baldwin, Wampler, & Gaskell 1989, hereafter BWG). This so-called “Baldwin Effect” is significant in that it might be used to determine the intrinsic luminosities and cosmological distances of these objects (e.g., Baldwin et al. 1978) and to probe the conditions near the central engine (Mushotzky & Ferland 1984). The Baldwin Effect is generally interpreted as arising from a decrease in ionization with an increase in luminosity (Mushotzky & Ferland 1984). Since this model can explain variations in UV line intensity ratios with luminosity also observed in quasars (Kinney et al. 1985, 1987; BWG), it is favored over models in which the emission lines are unrelated to the continuum flux (cf. Murdoch 1983; Netzer 1985).

We have found that the Baldwin Effect is not limited to active galactic nuclei (AGNs): our multiwavelength studies of Wolf-Rayet (W-R) stars reveal analogous inverse correlations between emission-line equivalent widths and the continuum luminosity. The strong, broad emission lines, which are formed at various depths in substantial winds, dominate the spectra of these objects (e.g., Conti & Massey 1989). The appearance of the lines defines the two W-R star sequences (e.g., Smith 1968): the WN sequence, where lines of helium and nitrogen dominate; and the WC sequence, in which carbon, helium, and oxygen lines are abundant. Ionization subtypes within each sequence follow various line ratios of nitrogen ions and of carbon ions for the WN and WC stars, respectively. In the WN stars of the Large Magellanic Cloud (LMC), where we have an assured luminosity from the well-known distance, we find a Baldwin Effect for a number of UV and optical emission lines.

2. OBSERVED TRENDS

Extinction-corrected continuum fluxes of the WN stars in the LMC are given in Morris et al. (1993). The UV resonance transitions appear as P Cygni lines in W-R stars, as opposed to pure emission in quasars; we have measured *only* the emission components here. The absolute continuum luminosity is determined using the LMC distance modulus 18.5 (Panagia et al. 1991). The quasar measurements are taken from Baldwin (1977), WGBB, and BWG; the observations for the different samples are described in these works and the references therein.

In Figure 1 we compare the Baldwin Effect in quasars to that of the LMC WN stars for the C IV $\lambda 1550$ resonance doublet. In W-R stars, the redshifted emission component of this transition originates from layers of the wind where the line is optically thick; its strength can be equaled and even exceeded by the blueshifted absorption component. The early (WNE) types generally produce stronger emission lines above fainter continua than do the late (WNL) types, behavior which persists in all of the lines examined here. Least-squares regression (LSR) fits are given in Table 1. Note that this limited sample of WN stars covers a wider luminosity range (3.0 dex) than does the set of quasars (2.4 dex), but they are separated (on average) by ~ 8 dex.¹

Figure 2 illustrates the Baldwin Effect for the N V $\lambda 1240$ resonance line in the WN stars. As for C IV, this transition occurs as a P Cygni line with strong absorption. In this case, however, the emission component dominates the overall line profile and therefore originates in layers which are less optically thick to the line radiation.

¹ We cannot resist pointing out that were the luminosity of quasars to be attributed *entirely* to WN stars (a “Terlevich Effect”), some 10^8 would be required on average.

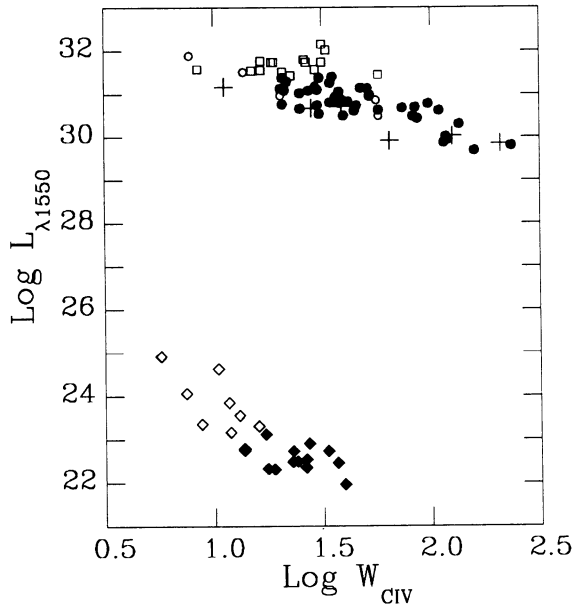


FIG. 1.—Log equivalent width (in Å) of C IV $\lambda 1550$ vs. the log continuum luminosity (in $\text{ergs s}^{-1} \text{Hz}^{-1}$) at 1550 Å for quasars and LMC WN stars. Discussion of the behavior exhibited by the different samples of quasars (circles, boxes, crosses) may be found in WGBB and BWG. Open and filled diamonds represent WNL and WNE stars, respectively. Fit statistics are given in Table 1.

Observed inverse correlations for the (mostly) pure emission He II recombination lines of $\lambda 1640$, $\lambda 4686$, and $\lambda 5411$ are plotted in Figure 3a–3c. Line and continuum predictions from the non-LTE, isotropic helium atmospheres (representative of WN stars) of Hamann & Schmutz (1987, hereafter HS), Schmutz, Hamann, & Wessolowski (1989, hereafter SHW), and Schmutz et al. (1993) are consistent with the observed relations. Model predictions for He II $\lambda\lambda 1640$, 4686, 5411 are plotted in Figure 3d–3f. Each datum corresponds to a model atmosphere specified by a “core” radius and the effective temperature T_* (see, e.g., SHW), where the different symbols identify temperatures in the range 35,000–90,000 K. No dependence on T_* is obvious here, but we do find a smooth transition in wind density: models with strong lines and faint continua are identi-

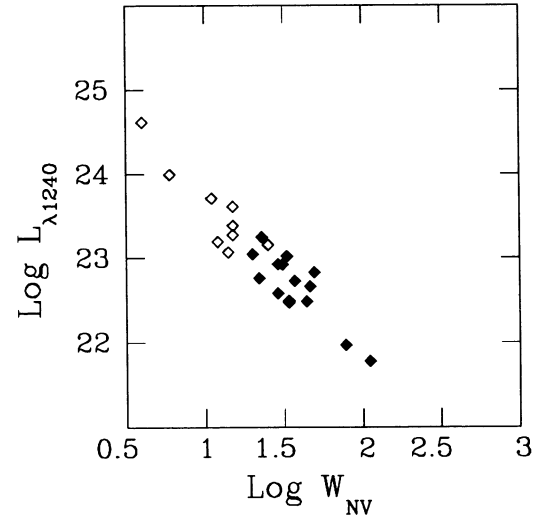


FIG. 2.—Log equivalent width and log continuum luminosity for N v $\lambda 1240$. Units and symbols are the same as Fig. 1; fits to the points are found in Table 1.

fied as having the smallest radii, indicating almost immediately that the *Baldwin Effect arises primarily from a difference in wind density among stars*. A wide range of flux in each transition is spanned by these models so that the Effect cannot be attributed to a variation of the continuum luminosity alone. This fact is consistent with the observations: the intrinsic fluxes of, e.g., the He II $\lambda 1640$ line are distributed over ~ 1.5 dex in the stars of the present data set.

Our use of the detailed models warrants a cautionary note. The predictions by HS and SHW are made for models with a constant mass-loss rate, \dot{M} , and constant terminal velocity of the wind, v_∞ . Since the density of the wind scales as $\dot{M}/v_\infty R_*^2$, the variations in density of the models is only due to the variation of R_* . In reality the value of \dot{M}/v_∞ varies from star to star.

3. AN EXPLANATION FOR THE BALDWIN EFFECT OF THE He II LINES

The Baldwin Effect for He II emission lines in the spectra of W-R stars can be understood if we make two assumptions:

TABLE 1
BALDWIN EFFECT LSR FIT PARAMETERS^a

Ion	a	σ_a	b	σ_b	$\sigma_{\log L}$ (dex)	Remarks
LMC WN Stars						
N v $\lambda 1240$	1.77	0.14	25.43	0.20	0.22	Strong P Cygni absorption
C iv $\lambda 1550$	2.79	0.43	26.48	0.53	0.44	Very strong P Cygni absorption
He II $\lambda 1640$	1.33 (1.38)	0.14 (0.06)	25.39 (25.56)	0.26 (0.09)	0.34 (0.10)	
N iv $\lambda 1718$	2.05	0.18	25.42	0.23	0.22	Moderate P Cygni absorption
He II $\lambda 3203$	1.63	0.19	26.48	0.53	0.36	...
He II $\lambda 4686$	1.14 (1.39)	0.19 (0.13)	25.04 (25.80)	0.42 (0.25)	0.34 (0.20)	...
He II $\lambda 5411$	1.19 (1.23)	0.19 (0.06)	24.28 (24.68)	0.30 (0.09)	0.30 (0.14)	...
He II $\lambda 10124$	1.36	0.18	23.99	0.44	0.27	...
QSO						
C iv $\lambda 1550$	1.42	0.14	33.22	0.22	0.36	...

^a The parameters a and b are specified by $\log L_\lambda = b - a \log W_\lambda$, where L_λ is in units of $\text{ergs s}^{-1} \text{Hz}^{-1}$ and W_λ is in Å. Values in parentheses are derived from model helium atmosphere predictions (see text and Fig. 3).

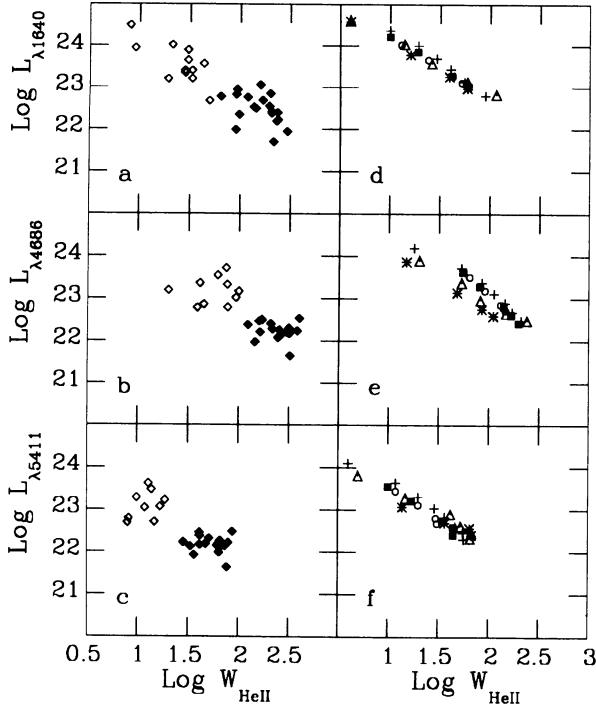


FIG. 3.—Log equivalent width and log continuum luminosity for the observed WN star He II transitions at (a) 1640 Å, (b) 4686 Å, and (c) 5411 Å, where diamonds are the same as in Fig. 1. Panels (d–f) illustrate the Effect as predicted from non-LTE pure helium model atmospheres for constant mass loss (see text), scaled to the LMC distance of 50.1 kpc. Symbols identify “effective” temperatures: 35 kK (open circles); 45 kK (filled boxes); 55 kK (crosses); 75 kK (triangles); and 90 kK (stars). Fit statistics are found in Table 1.

(1) the continuum is due primarily to free-free and bound-free opacity and (2) the major contribution to the equivalent width is from layers in the wind which are optically thin for line radiation. The first assumption is justified by the high degree of ionization in the winds of W-R stars and by the fact that electron scattering hardly affects the continuum. The optical depth for electron scattering is larger than that for free-free absorption in the visual and UV, but electron scattering neither creates nor destroys photons, except those scattered back into the continuum forming region. Lamers & Waters (1984) have calculated the reduction of the continuum flux by electron scattering and found it to be negligible. The second assumption is justified by the high wind velocity of the W-R stars ($\sim 2000 \text{ km s}^{-1}$) and the large acceleration which reduces the optical depth of the lines in the Sobolev approximation. An increase in the wind density moves the radius where the continuum is formed further out into the wind, increasing the continuum flux. This reduces the emitting volume for the line radiation, although its emission measure increases. Therefore the line emission increases less than the continuum emission, so the equivalent width decreases with increasing wind density. We demonstrate this for the He II lines with a highly simplified wind model in which the continuum flux and line flux are expressed in terms of the stellar parameters.

The velocity in the wind is

$$v(r) = v_{\infty}(1 - R_{*}/r)^{\beta}. \quad (1)$$

The value of β is not critical to our explanation, but for numerical ease in solving the equations below we choose

$\beta = \frac{1}{2}$. We introduce the dimensionless parameters $x = r/R_{*}$ and $w(x) = v(r)/v_{\infty}$. We adopt a temperature which varies as $T = T_{*}x^{-1}$ for $x \leq 2$ and $T = T_{*}/2$ for $x \geq 2$. Helium is assumed to be twice ionized in the layers of the wind where the lines and the continuum are formed.

The luminosity of the continuum can be estimated by

$$L_{\lambda}^c \simeq 4\pi r_{1/3}^2 B_{\lambda}(T) \sim R_{*}^2 x_{1/3}^2 B_{\lambda}[T(x_{1/3})], \quad (2)$$

where $r_{1/3}$ is the radius where the radial optical depth for the continuum is $\tau_{\lambda}^c = \frac{1}{3}$ and $x_{1/3} = r_{1/3}/R_{*}$. When the continuum flux is due primarily to free-free and bound-free opacity, for which $\kappa_{\lambda} \sim n_e^2 T^{-\alpha}$ with $\alpha = \frac{3}{2}$ for $h\nu < kT$ and $\alpha = \frac{1}{2}$ for $h\nu > kT$, the location $x_{1/3}$ is given by the condition

$$\int_{x_{1/3}}^{\infty} x^{-4} w^{-2} (T/T_{*})^{-1/2} (1 - e^{-h\nu/kT}) dx \sim \lambda^{-2} (\dot{M}/v_{\infty})^{-2} R_{*}^3 T_{*}^{3/2}. \quad (3)$$

The dependence of the opacity on n_e^2 has been expressed in wind parameters through the mass continuity equation. We will use the values of $x_{1/3}$ together with equation (2) to estimate L_{λ}^c .

For the line emission we assume that the upper level of the transition is in LTE with respect to the next ionization stage or that the non-LTE departure coefficient is about constant in the wind. Hillier (1987) and de Koter et al. (1993) have shown that this is a reasonable assumption for He II levels of $b \geq 4$ within the first few stellar radii in the winds of W-R stars.

The line emission (l) of optically thin lines is

$$L^l = 4\pi A_{ul} h\nu \int_{r_{1/3}}^{\infty} n_u r^2 dr \sim \left(\frac{\dot{M}}{v_{\infty}}\right)^2 R_{*}^{-1} T_{*}^{-3/2} q_{i+1} \int_{x_{1/3}}^{\infty} x^{-2} w^{-2} \times \left(\frac{T}{T_{*}}\right)^{-3/2} e^{\chi_u/kT} (1 - e^{-h\nu/kT}) dx, \quad (4)$$

where A_{ul} is the Einstein coefficient, and the factor q_{i+1} is the ionization fraction of the next higher stage. We assume that helium is He^{++} , so $q_{i+1} = 1$. The number density n_u of the upper level of the observed transition is given by $n_u \sim n_e^2 b_u e^{\chi_u/kT} T^{-3/2}$, where χ_u is the ionization potential of the upper level and b_u is the constant departure coefficient. The layer where the continuum becomes optically thin at the wavelength of the line is found at $r_{1/3}$.

At long wavelengths ($h\nu < kT$) in the visual and near-IR we can approximate the integral of equation (3) by $\sim x_{1/3}^{-7/2}$ and the integral of equation (4) by $\sim x_{1/3}^{-7/6}$. These approximations are valid within $\sim 10\%$ in the range of $1.2 \leq x_{1/3} \leq 4$. We can also adopt the Rayleigh-Jeans limit of the Planck function, with $T(r_{1/3}) = T_{*}/x_{1/3}$. With this solution for $x_{1/3}$ we find

$$L_{\lambda}^c \sim (\dot{M}/v_{\infty})^{4/7} R_{*}^{8/7} T_{*}^{4/7}, \quad (5)$$

$$L^l \sim (\dot{M}/v_{\infty})^{4/3} R_{*}^0 T_{*}^{-2} e^{\chi_u/kT}, \quad (6)$$

$$W_{\lambda} \sim (\dot{M}/v_{\infty})^{16/21} R_{*}^{-8/7} T_{*}^{-5/2} e^{\chi_u/kT}. \quad (7)$$

For the He II $\lambda 5411$ line $\chi_u = 1.1 \text{ eV}$ so $e^{\chi_u/kT} \simeq 1$. These equations show that the powers of R_{*} and T_{*} are positive in L_{λ}^c and negative in W_{λ} , so there is an inverse relation between W_{λ} and L_{λ}^c among different W-R stars. If R_{*} is the dominant variable here then the predicted slope of the Baldwin relation is -1 , which is close to the observed value of -1.19 .

The expected slope would be $-8/35$ if T_* is the dominant variable, and $+3/4$ if (\dot{M}/v_∞) is the dominant variable. In reality, the slope is due to the combination of the variations of all these parameters, however, the main effect is due to the large variations in R_* .

For lines at shorter wavelengths such as the He II $\lambda 1640$ line the value of $\chi_u/kT \gg 1$ and the Wien approximation of the Planck function can be applied. This yields a slope of -2 for the relation between L_λ^c and W_λ through R_* . The temperature dependence is more complex than in the long-wavelength limit, but using $T \simeq T_*/2$ we find for the He II $\lambda 1640$ line ($\chi_u = 6$ eV) a temperature slope of -0.46 over the range $30,000 \text{ K} \leq T_* \leq 90,000 \text{ K}$. In reality the slope will be due to the variation of both T_* and R_* and is expected to be between -0.46 and -2 , which is in agreement with the observed value of -1.33 .

Although the simple model proposed here predicts about the right slopes for the He II lines, the assumption of a constant ionization factor q_{i+1} in the wind is not justified for high ionization lines such as N V $\lambda 1240$ and C IV $\lambda 1550$. Nor can we assume these lines to be optically thin due to their strong P Cygni absorption. In this case the dependence of q_{i+1} on the stellar parameters should be taken into account, but to do so is beyond the scope of this paper.

4. CONCLUSIONS

Since the WN star Baldwin Effect occurs for a number of lines, we have at our disposal a method which should yield accurate distances to WN stars in the Galaxy, provided that the relations can also be calibrated for stars of Galactic metallicity. The small spread in W_{NV} around the mean relation implies an uncertainty in the distance determination of only 0.15 dex. The distances and a more detailed theoretical treatment are the subject of current work.

Our understanding of the phenomenon in W-R stars may yield some insight on physical origin of the Effect in quasars. The problem is that the "standard model" of AGNs (reviewed by Blanford & Rees 1992) bears little resemblance to the typical held view of W-R stars. Continuum emission from AGNs is generally explained using various accretion disk models with the underlying hypothesis that the emission emerges from the gravitational potential well produced by a massive black hole in the center of the galaxy. An alternative

interpretation for the activity of AGNs is the starburst model (Terlevich et al. 1987) in which the nuclear activity arises from the coeval evolution of a young, dense cluster of massive stars in the high metal abundance nuclear regions of early-type galaxies (Diaz et al. 1985). This scenario has been applied with some success to the broad-line regions of lower luminosity AGNs (Terlevich et al. 1992). But there exists a distinct observational difference between the continua of quasars and W-R stars: while both can be represented by a power law $F_\lambda \sim \lambda^{-\alpha}$ (Morris et al. 1993; BWG), the average values of α are the same in magnitude (≈ 3) but *opposite* in sign (the fluxes from W-R stars decrease with increasing λ). Broad line emission from AGNs occurs in gas clouds for which there is a large range of internal velocities, although there appears to be a net outward flow of mass (see, e.g., Osterbrock 1993 and the references therein).

Ferland et al. (1992) gives evidence for an ionization structure in the clouds, for the continuum and line-forming regions being closer together than previously believed, producing an appreciable range of temperatures and densities in the line-forming region. It is plausible that the quasar Baldwin Effect is explainable in terms of an outward decreasing temperature and large variations in densities in which the lines are optically thin due to a large velocity gradient. In the present model, the relatively shallow slope for the quasar C IV $\lambda 1550$ line (Table 1) would suggest that the line is emitted mostly from layers that are optically thin. The radiation density in the clouds is very high (Peterson 1988), however, meaning that large column densities are required to make the ionizing continuum optically thick and thus produce a range of emission-line strengths. As a consequence, the lines should also be optically thick (Ferland et al. 1992). In this case, the difference in slopes between the quasar and WN star C IV $\lambda 1550$ slopes could be due to the strong P Cygni absorption components in the WN stars.

We appreciate the comments of J. Baldwin, E. Gosset, G. Ferland, and M. van Kerkwijk. We also thank our referee, P. Massey, and L. Volsky at JILA for her editorial assistance. This work is supported by research grants from NASA (grant NAG5-1016) and the National Science Foundation (grant AST 90-15240).

REFERENCES

- Baldwin, J. A. 1977, *ApJ*, 214, 679
 Baldwin, J. A., Burke, W. L., Gaskell, C. M., & Wampler, E. J. 1978, *Nature*, 273, 431
 Baldwin, J. A., Wampler, E. J., & Gaskell, C. M. 1989, *ApJ*, 338, 630 (BWG)
 Blandford, R. D., & Rees, M. J. 1992, in *Testing the AGN Paradigm*, ed. S. S. Holt, S. G. Neff, & C. M. Urry (New York: AIP), 3
 Conti, P. S., & Massey, P. 1989, *ApJ*, 337, 251
 de Koter, A., Schmutz, W., & Lamers, H. J. G. L. M. 1993, *A&A*, in press
 Diaz, A., Pagel, G. E. J., & Wilson, I. 1985, in *Active Galactic Nuclei*, ed. J. E. Dyson (Manchester Univ. Press), 171
 Ferland, G. J., Peterson, B. M., Horne, K., Welsh, W. F., & Nahar, S. N. 1992, *ApJ*, 387, 95
 Hamann, W.-R., & Schmutz, W. 1987, *A&A*, 174, 173 (HS)
 Hillier, D. J. 1987, *ApJ*, 63, 947
 Kinney, A. L., Huggins, P. J., Bregman, J. N., & Glassgold, A. E. 1985, *ApJ*, 291, 128
 Kinney, A. L., Huggins, P. J., Glassgold, A. E., & Bregman, J. N. 1987, *ApJ*, 314, 128
 Lamers, H. J. G. L. M., & Waters, L. B. F. M. 1984, *A&A*, 136, 37
 Morris, P. W., Brownsberger, K. R., Conti, P. S., Massey, P., & Vacca, W. D. 1993, *ApJ*, in press
 Murdoch, H. S. 1983, *MNRAS*, 202, 987
 Mushotzky, R., & Ferland, G. J. 1984, *ApJ*, 278, 558
 Netzer, H. 1985, *MNRAS*, 216, 63
 Osterbrock, D. E. 1993, *ApJ*, 404, 551
 Panagia, N., Gilmozzi, R., Macchetto, F., Adorf, H.-M., & Kirshner, R. P. 1991, *ApJ*, 380, L23
 Peterson, B. M. 1988, *PASP*, 100, 18
 Schmutz, W., Hamann, W.-R., & Wessolowski, U. 1989, *A&A*, 210, 236 (SHW)
 Schmutz, W., Vogel, M., Hamann, W.-R., & Wessolowski, U. 1993, in preparation
 Smith, L. F. 1968, *MNRAS*, 140, 409
 Terlevich, R., Melnick, J., & Moles, M. 1987, in *Observational Evidence for Activity in Galaxies*, ed. E. Ye. Khachiyani, K. J. Fricke, & J. Melnick (Dordrecht: Reidel), 499
 Terlevich, R., Tenorio-Tagle, G., Franco, J., & Melnick, J. 1992, *MNRAS*, 255, 713
 Wampler, E. J., Gaskell, C. M., Burke, W. L., & Baldwin, J. A. 1984, *ApJ*, 276, 403 (WGBB)